Last orbits of binary strange quark stars

Francois Limousin, Dorota Gondek-Rosinska, Eric Gourgoulhon

Last orbits of binary strange quark stars

François Limousin,[1,*] Dorota Gondek-Rosińska,[1,2,3,4,†] and Eric Gourgoulhon[1,‡]

[1] *Laboratoire de l'Univers et de ses Théories, UMR 8102 du C.N.R.S., Observatoire de Paris, Université Paris 7, F-92195 Meudon Cedex, France*
[2] *Nicolaus Copernicus Astronomical Center, Bartycka 18, 00-716 Warszawa, Poland*
[3] *Departament de Fisica Aplicada, Universitat d'Alacant, Apartat de correus 99, 03080 Alacant, Spain*
[4] *Institute of Astronomy, University of Zielona Góra, Lubuska 2, 65-265, Zielona Góra, Poland*

We present the first relativistic calculations of the final phase of inspiral of a binary system consisting of two stars built predominantely of strange quark matter (strange quark stars). We study the precoalescing stage within the Isenberg-Wilson-Mathews approximation of general relativity using a multidomain spectral method. A hydrodynamical treatment is performed under the assumption that the flow is either rigidly rotating or irrotational, taking into account the finite density at the stellar surface — a distinctive feature with respect to the neutron star case. The gravitational-radiation driven evolution of the binary system is approximated by a sequence of quasi-equilibrium configurations at fixed baryon number and decreasing separation. We find that the innermost stable circular orbit (ISCO) is given by an orbital instability both for synchronized and irrotational systems. This constrasts with neutron stars for which the ISCO is given by the mass-shedding limit in the irrotational case. The gravitational wave frequency at the ISCO, which marks the end of the inspiral phase, is found to be ~ 1400 Hz for two irrotational $1.35\,M_\odot$ strange stars and for the MIT bag model of strange matter with massless quarks and a bag constant $B = 60$ MeV fm^{-3}. Detailed comparisons with binary neutrons star models, as well as with third order Post-Newtonian point-mass binaries are given.

PACS numbers: 04.40.Dg, 04.30.Db, 04.25.Dm, 97.10.Kc, 97.60.Jd

I. INTRODUCTION

One of the most important prediction of general relativity is gravitational radiation. Coalescing neutron star binaries are considered among the strongest and most likely sources of gravitational waves to be seen by VIRGO/LIGO interferometers [1, 2]. Due to the emission of gravitational radiation, binary neutron stars decrease their orbital separation and finally merge. Gravitational waves emitted during the last few orbits of inspiral could yield important informations about the equation of state (EOS) of dense matter [3, 4, 5, 6]. With accurate templates of gravitational waves from coalescing binary compact stars, it may be possible to extract information about physics of neutron stars from signals observed by the interferometers and to solve one of the central but also most complex problem of physics — the problem of the absolute ground state of matter at high densities. It is still an open question whether the core of a neutron star consists mainly of superfluid neutrons or exotic matter like strange quark matter, pions or kaons condensates (see e.g. Ref. [7] for a recent review). The possibility of the existence of quark matter dates back to the early seventies. Bodmer [8] remarked that matter consisting of deconfined up, down and strange quarks could be the absolute ground state of matter at zero pressure and temperature. If this is true then objects made of such matter, the so-called *strange stars*, could exist [9, 10, 11]. Strange quark stars are currently considered as a possible alternative to neutron stars as compact objects (see e.g. [12, 13, 14] and references therein).

The evolution of a binary system of compact objects is entirely driven by gravitational radiation and can be roughly divided into three phases : point-like inspiral, hydrodynamical inspiral and merger. The first phase corresponds to large orbital separation (much larger than the neutron star radius) and can be treated analytically using the post-Newtonian (PN) approximation to general relativity (see Ref. [15] for a review). In the second phase the orbital separation becomes only a few times larger than the radius of the star, so the effects of tidal deformation, finite size and hydrodynamics play an important role. In this phase, since the shrinking time of the orbital radius due to the emission of gravitational waves is still larger than the orbital period, it is possible to approximate the state as quasi-equilibrium [16, 17]. The final phase of the evolution is the merger of the two objects, which occur dynamically [18, 19, 20, 21]. Note that quasi-equilibrium computations from the second phase provide valuable initial data for the merger [5, 18, 20, 22].

Almost all studies of the final phase of the inspiral of close binary neutron star systems employ a simplified EOS of dense matter, namely a polytropic EOS [3, 4, 17, 22, 23, 24, 25, 26, 27, 28]. There are only two exceptions: (i) Oechslin et al. have used a pure nuclear matter EOS, based on a relativistic mean field model and a 'hybrid' EOS with a phase transition to quark matter at high density [5]; (ii) Bejger et al. have computed quasi-equilibrium sequences based on three nuclear mat-

*Francois.Limousin@obspm.fr
†Dorota.Gondek@obspm.fr
‡Eric.Gourgoulhon@obspm.fr

ter EOS [6]. In this article we present results on the hydrodynamical phase of inspiraling binary strange quark stars described by MIT bag model. The calculations are performed in the framework of *Isenberg-Wilson-Mathews* approximation to general relativity (see Ref. [29] for a review). We consider binary systems consisting of two identical stars. We choose the gravitational mass of each star to be $1.35\,M_\odot$ in infinite separation in order to be consistent with recent population synthesis calculations [30] and with the current set of well-measured neutron star masses in relativistic binary radio pulsars [31, 32]. We compare the evolution of a strange star binary system with a neutron star binary in order to find any characteristic features in the gravitational waveform that will help to distinguish between strange stars and neutron stars. We consider two limiting cases of velocity flow in stellar interior: the irrotational and the synchronized case in order to exhibit the differences between these two extreme states. The irrotational case is more realistic since the viscosity of neutron star matter (or strange star matter) is far too low to ensure synchronization during the late stage of the inspiral [33, 34]. Due to the finite density at the surface of bare strange stars, we had to introduce a treatment of the boundary condition for the velocity potential (in the irrotational case) different from that of neutron stars, where the density vanishes at the stellar surface.

The paper is organized in the following way: Sec. II is a brief summary of the assumptions upon which this work is based, Sec. III is devoted to the description of the EOS used to describe strange stars and neutron stars. In Sec. IV we briefly describe the basic equations for quasi-equilibrium and derive the boundary condition required for solving the fluid equation of irrotational flow with finite surface density, which is relevant for strange stars. In Sec. V we present the numerical results for corotating and irrotational strange stars binaries and compare their quasistationary evolution with that of neutron stars, as well as with that of post-Newtonian point-masses. Section VI contains the final discussion. Throughout the paper, we use geometrized units, for which $G = c = 1$, where G and c denote the gravitational constant and speed of light respectively.

II. ASSUMPTIONS

The first assumption regards the matter stress-energy tensor $\boldsymbol{T}$, which we assume to have the **perfect fluid** form:

$$\boldsymbol{T} = (e + p)\boldsymbol{u} \otimes \boldsymbol{u} + p\,\boldsymbol{g}, \tag{1}$$

where e, p, $\boldsymbol{u}$ and $\boldsymbol{g}$ are respectively the fluid proper energy density, the fluid pressure, the fluid 4-velocity, and the spacetime metric. This is a very good approximation for neutron star matter or strange star matter.

The last orbits of inspiraling binary compact stars can be studied in the **quasi-equilibrium** approximation. Under this assumption the evolution of a system is approximated by a sequence of exactly circular orbits. This assumption results from the fact that the time evolution of an orbit is still much larger than the orbital period and that the gravitational radiation circularizes an orbit of a binary system. This implies a continuous spacetime symmetry, called *helical symmetry* [35, 36] represented by the Killing vector:

$$\boldsymbol{\ell} = \frac{\partial}{\partial t} + \Omega \frac{\partial}{\partial \varphi}, \tag{2}$$

where Ω is the orbital angular velocity and $\partial/\partial t$ and $\partial/\partial\varphi$ are the natural frame vectors associated with the time coordinate t and the azimuthal coordinate φ of an asymptotic inertial observer.

One can then introduce the *shift vector* $\boldsymbol{B}$ of coorbiting coordinates by means of the orthogonal decomposition of $\boldsymbol{\ell}$ with respect to the Σ_t foliation of the standard 3+1 formalism:

$$\boldsymbol{\ell} = N\,\boldsymbol{n} - \boldsymbol{B}, \tag{3}$$

where $\boldsymbol{n}$ is the unit future directed vector normal to Σ_t, N is called the *lapse function* and $\boldsymbol{n} \cdot \boldsymbol{B} = 0$.

We also assume that the spatial part of the metric (i.e. the metric induced by $\boldsymbol{g}$ on each hypersurface Σ_t) is conformally flat, which corresponds to the **Isenberg-Wilson-Mathews** (IWM) approximation to general relativity [37, 38, 39] (see Ref. [36] for a discussion). Thanks to this approximation we have to solve only five of the ten Einstein equations. In the IWM approximation, the spacetime metric takes the form:

$$ds^2 = -(N^2 - B_i B^i)dt^2 - 2B_i\,dt\,dx^i + A^2 f_{ij} dx^i dx^j, \tag{4}$$

where A is some conformal factor, f_{ij} the flat spatial metric and Latin indices run in $\{1, 2, 3\}$ (spatial indices). The comparison between the IWM results presented here and the non-conformally flat ones will be performed in a future article [40].

The fourth assumption concerns the fluid motion inside each star. We consider two limiting cases: **synchronized** (also called corotating) motion and **irrotational** flow (assuming that the fluid has zero vorticity in the inertial frame). The latter state is more realistic.

We consider only **equal-mass** binaries consisting of identical stars with gravitational masses $M_1 = M_2 = 1.35\ M_\odot$ measured in infinite separation. The main reason for choosing these particular masses is that five out of six observed binary radio pulsars have mass ratio close to unity and gravitational masses of each star $\sim 1.3{-}1.4 M_\odot$ [31, 32]. In addition population synthesis calculations [30] have shown that a significant fraction of the observed binary neutron stars in gravitational waves will contain stars with equal masses $\sim 1.4\ M_\odot$ and systems consisting of a low and a high mass neutron star.

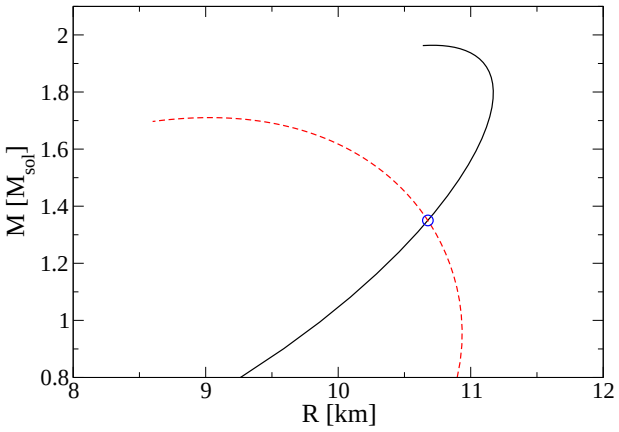

FIG. 1: Gravitational mass M versus areal radius R for sequences of static strange quark stars described by the simplest MIT bag model (solid line) and neutron stars described by polytropic EOS with $\gamma = 2.5$ and $\kappa = 0.0093\ m_0\, n_{\rm nuc}^{1.5}$ (dashed line). The two sequences are crossing at the point $M = 1.35\ M_\odot$ and $R = 10.677$ km (marked by a circle).

III. THE EQUATION OF STATE AND STELLAR MODELS

It has been shown [3, 4] that the evolution of equal-mass binary neutron stars depend mainly on the compactness parameter M/R, where M and R are the gravitational mass measured by an observer at infinity for a single isolated neutron star and the stellar radius respectively. It is therefore interesting to check if the properties of inspiraling strange stars can be predicted by studying binaries consisting of polytropic neutron stars having the same mass and the same compactness parameter. Therefore we perform calculations for two different equations of state of dense matter: a strange quark matter EOS and a polytropic EOS.

Typically, strange stars are modeled [10, 11] with an equation of state based on the MIT-bag model of quark matter, in which quark confinement is described by an energy term proportional to the volume [41]. The equation of state is given by the simple formula

$$p = a(\rho - \rho_0), \tag{5}$$

$$n(p) = n_0 \cdot \left[1 + \frac{1+a}{a}\frac{p}{\rho_0}\right]^{1/(1+a)}, \tag{6}$$

where n is the baryon density and $a,\ \rho_0, n_0$ are some constants depending on the 3 parameters of the model (the bag constant B, the mass of the strange quarks $m_{\rm s}$ and the strenght of the QCD coupling constant α). In general this equation corresponds to a self-bound matter with mass density ρ_0 and baryon density n_0 at zero pressure and with a fixed sound velocity ($\sqrt{a}$) at all pressures. It was shown that different strange quark models can be approximated very well by Eqs (5) and (6) [42, 43].

In the numerical calculations reported in the present paper we describe strange quark matter using the simplest MIT bag model (with massless and non-interacting quarks), for which the formula (5) is exact. We choose the value of the bag constant to be $B = 60$ MeV fm^{-3}. For this model we have $a = 1/3$, $\rho_0 = 4.2785 \times 10^{14}$ g cm^{-3} and $n_0 = 0.28665$ fm^{-3}. In general for the MIT bag model the density of strange quark matter at zero pressure is in the range $\sim 3 \times 10^{14} - 6.5 \times 10^{14}$ g cm^{-3} and a between 0.289 and 1/3 (for $0 \le \alpha \le 0.6$ and $0 \le m_{\rm s} \le 250$ MeV) [43]. The higher value of a and of ρ_0 the higher compactness parameter of a star with fixed gravitational mass.

Up to now, the majority of calculations of the hydrodynamical inspiral phase [3, 4, 17, 22, 23, 24, 25, 26, 27, 28] and all calculations of the merger phase [18, 19, 20, 21] have been performed for binary systems containing neutron stars described by a polytropic EOS:

$$p = \kappa n^\gamma, \tag{7}$$

where κ and γ coefficients are some constant numbers: κ represents the overall compressibility of matter while γ measures the stiffness of the EOS. The total energy density is related to the baryon density by

$$e(n) = \frac{\kappa}{\gamma - 1} n^\gamma + \mu_0\, n\ , \tag{8}$$

where μ_0 is the chemical potential at zero pressure.

In order to compare results for strange stars with those for neutron stars, we determine the values of κ and γ which yield to the same radius for the gravitational mass $M = 1.35\, M_\odot$ as that obtained for a static strange star. It was shown [6] that the properties of inspiraling neutron stars described by realistic EOS can be, in a good approximation, predicted by studying binaries with assumed polytropic EOSs with $\gamma = 2$ or 2.5. For a 1.35 $M_\odot$ strange star we have a high value of compactness parameter $M/R = 0.1867$ so we have choosen $\gamma = 2.5$, for which we found $\kappa = 0.00937\ m_0\, n_{\rm nuc}^{1.5}$, with the rest mass of relativistic particles $m_0 := 1.66 \times 10^{-27}$ kg and $n_{\rm nuc} = 0.1$ fm^{-3}.

In Fig. 1 we present the mass-radius relation for a sequence of static stars described by the simplest MIT bag model (solid line) and the polytropic EOS (dashed line) parametrized by central density. For small mass strange stars $M \sim R^3$ since density is almost constant inside a star $\sim \rho_0$. In the top panel of Fig. 2 we show the mass density distribution inside the strange star (solid line) and the neutron star described by polytropic EOS (dashed line) having gravitational mass 1.35 $M_\odot$ and areal radius 10.667 km (the configurations corresponding to the crossing point on Fig. 1). The huge density jump at the surface of the strange star corresponds to $\rho_0 = 4B$. The value of density at the surface describes strongly or weakly bound strange matter, which in each case must be absolutely stable with respect to ^{56}Fe.

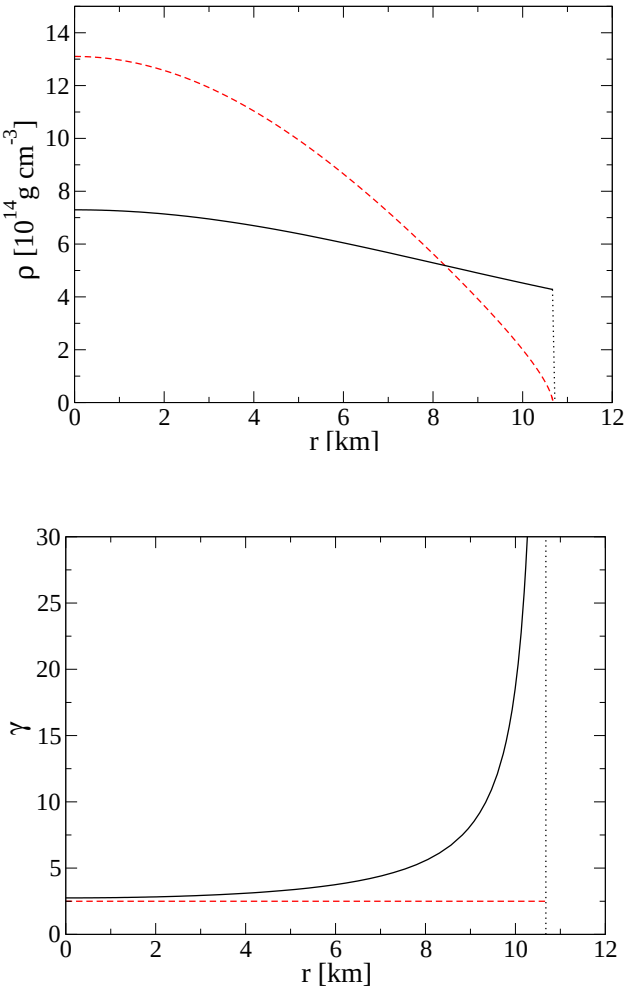

FIG. 2: Mass density (top panel) and the adiabatic index γ (bottom panel) versus the radial coordinate r for a static strange quark star (solid line) and a polytropic neutron star (dashed line), having both a gravitational mass of 1.35 $M_\odot$ and an areal radius $R = 10.677$ km (resulting in the compactness parameter $M/R = 0.1867$). The vertical dotted line corresponds to the stellar surface.

An important quantity relevant for evolution of binary compact stars is the adiabatic index:

$$\gamma = \mathrm{d}\ln p/\mathrm{d}\ln n. \tag{9}$$

We assume that matter is catalized so the adiabatic index can be calculated directly from EOS (see Refs. [44] and [45] for discussion on different kind of adiabatic indices and corresponding timescales). Note that for the polytropic EOS given by Eq. (7) the index γ coincides with the adiabatic index of a relativistic isentropic fluid. Dependence of the adiabatic index γ on stellar radii for both EOS is shown in the bottom pannel of Fig. 2. The adiabatic index of strange matter is qualitatively different from the adiabatic index for polytropic EOS or for realistic EOS. The values of γ in the outer layers of strange stars are very large and for $\rho \to \rho_0$ we have $\gamma = a + \rho/(\rho - \rho_0) \to \infty$. The EOS of neutron stars for densities lower than $\sim 10^{14}$ g cm^{-3} (the crust) is well established [7]. In the outer crust of an ordinary neutron star the pressure is dominated by the ultra-relativistic electron gas, so we have $\gamma = 4/3$. The values of the local adiabatic index in the inner crust of a neutron star depends strongly on density and varies from $\gamma \simeq 0.5$ near the neutron drip point to $\gamma \simeq 1.6$ in the bottom layers near the crust-core interface.

In our calculations we use equation of state in the form:

$$n = n(H), \qquad e = e(H), \qquad p = p(H), \tag{10}$$

where H is pseudo-enthalpy (the log-enthalpy) defined by:

$$H(n) := \ln\left(\frac{e+p}{nE_0}\right), \tag{11}$$

where the energy per unit baryon number is $E_0 = m_0$ for a polytropic EOS, and $E_0 = \rho_0/n_0 = 837.26$ MeV for strange quark model described above. For our model of strange quark matter we have:

$$\rho = \rho_0(3\mathrm{e}^{4H}+1)/4, \quad p = \rho_0(\mathrm{e}^{4H}-1)/4\,, \quad n = n_0\mathrm{e}^{3H} \tag{12}$$

IV. EQUATIONS TO BE SOLVED

We refer the reader to Ref. [46] for the derivation of the equations describing quasi-equilibrium binary stars within the IWM approximation to general relativity. After recalling these equations, we mainly concentrate on the equation for the velocity potential of irrotational flows. Actually this equation has a different structure for strange stars than for neutron stars. This results from the non-vanishing of the density at the stellar surfaces of strange stars (cf. the top panel in Fig. 2).

A. The gravitational field equations

The gravitational field equations have been obtained within the 3+1 decomposition of the Einstein's equations [47, 48], taking into account the helical symmetry of spacetime. The trace of the spatial part of the Einstein equations combined with the Hamiltonian constraint results in two equations:

$$\underline{\Delta}\nu = 4\pi A^2(E+S) + A^2K_{ij}K^{ij} - \overline{\nabla}_i\nu\overline{\nabla}^i\beta, \tag{13}$$

$$\underline{\Delta}\beta = 4\pi A^2 S + \frac{3}{4}A^2K_{ij}K^{ij} - \frac{1}{2}(\overline{\nabla}_i\nu\overline{\nabla}^i\nu + \overline{\nabla}_i\beta\overline{\nabla}^i\beta), \tag{14}$$

where $\overline{\nabla}_i$ stands for the covariant derivative associated with the flat 3-metric f_{ij} and $\underline{\Delta} := \overline{\nabla}^i\overline{\nabla}_i$ for the associated Laplacian operator. The quantities ν and β are

defined by $\nu := \ln N$ and $\beta := \ln(AN)$, and K_{ij} denotes the extrinsic curvature tensor of the $t = $ const hypersurfaces. E and S are respectively the matter energy density and the trace of the stress tensor, both as measured by the observer whose 4-velocity is n^μ *(Eulerian observer)*:

$$E := T_{\mu\nu} n^\mu n^\nu, \tag{15}$$

$$S := A^2 f^{ij} T_{ij}. \tag{16}$$

In addition, we have also to solve the momentum constraint, which writes

$$\underline{\Delta} N^i + \frac{1}{3}\overline{\nabla}^i(\overline{\nabla}_j N^j) = -16\pi N A^2 (E+p) U^i + 2NA^2 K^{ij}\overline{\nabla}_j(3\beta - 4\nu), \tag{17}$$

where $N^i := B^i + \Omega(\partial/\partial\varphi)^i$ denotes the shift vector of nonrotating coordinates, and U^i is the fluid 3-velocity.

B. The fluid equations

Apart from the gravitational field equations, we have to solve the fluid equations. The equations governing the quasi-equilibrium state are the relativistic Euler equation and the equation of baryon number conservation. Both cases of irrotational and synchronized motions admit a first integral of the relativistic Euler equation:

$$H + \nu - \ln\Gamma_0 + \ln\Gamma = \text{const.}, \tag{18}$$

where Γ_0 is the Lorentz factor between the co-orbiting observer and the Eulerian observer and Γ is the Lorentz factor between the fluid and the co-orbiting observers ($\Gamma = 1$ for synchronized binaries).

For a synchronized motion, the equation of baryon number conservation is trivially satisfied, whereas for an irrotational flow, it is written as

$$\zeta H \underline{\Delta}\Psi + \overline{\nabla}^i H \overline{\nabla}_i \Psi = A^2 h \Gamma_{\rm n} U_0^i \overline{\nabla}_i H + \zeta H \times [\overline{\nabla}^i \Psi \overline{\nabla}_i (H-\beta) + A^2 h U_0^i \overline{\nabla}_i \Gamma_{\rm n}], \tag{19}$$

where Ψ is the velocity potential, $h := \exp(H)$, ζ the thermodynamical coefficient:

$$\zeta := \frac{d\ln H}{d\ln n}, \tag{20}$$

and $\Gamma_{\rm n}$ denotes the Lorentz factor between the fluid and the Eulerian observer and U_0^i is the orbital 3-velocity with respect to the Eulerian observers:

$$U_0^i = -\frac{B^i}{N}. \tag{21}$$

The fluid 3-velocity U^i with respect to the Eulerian observer is equal to U_0^i for synchronized binary systems, whereas

$$U^i = \frac{1}{A^2\Gamma_{\rm n} h}\overline{\nabla}^i \Psi \tag{22}$$

for irrotational ones.

C. Boundary condition for the velocity potential

The method of solving the elliptic equation (19) for the velocity potential is different for neutron stars and strange stars. In the case of neutron stars, the coefficient ζH in front of the Laplacian vanishes at the surface of the star so Eq. (19) is not merely a Poisson type equation for Ψ. It therefore deserves a special treatment (see Appendix B in [26] for a discussion). In the case of strange stars, the coefficient $\zeta H = 1/3$ in whole star so we have to deal with a usual Poisson equation and consequently we have to impose a boundary condition for the velocity potential at the stellar surface.

We can define the surface of the star by $n_{|\rm surf} = n_0 =$ constant. The surface of the fluid ball is obviously Lie-dragged along the fluid 4-velocity vector $\boldsymbol{u}$, so that this last condition gives

$$(\pounds_{\boldsymbol{u}} n)\big|_{\rm surf} = 0, \tag{23}$$

where $\pounds_{\boldsymbol{u}}$ is the Lie derivative along the vector field $\boldsymbol{u}$. Let us decompose $\boldsymbol{u}$ in a part along the helical Killing vector $\boldsymbol{\ell}$ and a part $\boldsymbol{S}$ parrallel to the hypersurface Σ_t:

$$\boldsymbol{u} = \lambda(\boldsymbol{\ell} + \boldsymbol{S}). \tag{24}$$

The condition (23) is then equivalent to

$$\lambda(\pounds_{\boldsymbol{\ell}} n + \pounds_{\boldsymbol{S}} n)\big|_{\rm surf} = 0. \tag{25}$$

Now, if the fluid flows obeys to the helical symmetry $\pounds_{\boldsymbol{\ell}} n = 0$; inserting this relation into Eq. (25) leads to $(\pounds_{\boldsymbol{S}} n)\big|_{\rm surf} = 0$ or equivalently (since $\boldsymbol{S}$ is a spatial vector):

$$(S^i \overline{\nabla}_i n)\big|_{\rm surf} = 0. \tag{26}$$

Now, let us express $\boldsymbol{S}$ in terms of the spatial vectors $\boldsymbol{U}$ and $\boldsymbol{B}$. First, Eq. (24) implies $\boldsymbol{n}\cdot\boldsymbol{u} = \lambda \boldsymbol{n}\cdot\boldsymbol{\ell}$. Secondly, the fluid motion $\boldsymbol{u}$ can be described by the orthogonal decomposition $\boldsymbol{u} = \Gamma_{\rm n}(\boldsymbol{n} + \boldsymbol{U})$ which yields $\boldsymbol{n}\cdot\boldsymbol{u} = -\Gamma_n$. Finally, from Eq. (3), we have $\boldsymbol{n}\cdot\boldsymbol{\ell} = -N$ so that the factor λ can be expressed as $\lambda = \Gamma_n/N$ and Eq. (24) becomes

$$\boldsymbol{u} = \frac{\Gamma_n}{N}(\boldsymbol{\ell} + \boldsymbol{S}). \tag{27}$$

Now, combining Eq. (27) and Eq. (3), we have

$$\boldsymbol{u} = \Gamma_n \left[\boldsymbol{n} + \frac{1}{N}(\boldsymbol{S} - \boldsymbol{B})\right]. \tag{28}$$

Comparing with the orthogonal decomposition $\boldsymbol{u} = \Gamma_{\rm n}(\boldsymbol{n} + \boldsymbol{U})$, we deduce that $\boldsymbol{S} = N\boldsymbol{U} + \boldsymbol{B}$. Inserting this relation into Eq. (26) leads to the boundary condition

$$(NU^i \overline{\nabla}_i n + B^i \overline{\nabla}_i n)\big|_{\rm surf} = 0. \tag{29}$$

Now, using Eq. (22), we obtain a Neumann-like boundary condition for Ψ:

$$(\overline{\nabla}^i n \overline{\nabla}_i \Psi)\Big|_{\rm surf} = -\left(\frac{\Gamma_n h A^2}{N} B^i \overline{\nabla}_i n\right)\Big|_{\rm surf}. \tag{30}$$

Considering the elliptic equation (19) for Ψ we see that the boundary condition we have obtained is consistent with the case $n = 0$ (or equivalently $\zeta H = 0$) at the stellar surface since, from Eq. (20), $\overline{\nabla}^i H = \frac{\zeta H}{n} \overline{\nabla}^i n$.

V. NUMERICAL RESULTS

A. The method

The resolution of the above nonlinear elliptic equations is performed thanks to a numerical code based on multidomain spectral methods and constructed upon the LORENE C++ library [51]. The detailed description of the whole algorithm, as well as numerous tests of the code can be found in [46]. Additional tests have been presented in Sec. 3 of [4]. The code has already been used successfully for calculating the final phase of inspiral of binary neutron stars described by polytropic EOS [4, 17, 27, 49, 50] and realistic EOS [6]. It is worth to stress that the adaptation of the domains (numerical grids) to the stellar surface (surface-fitted coordinates) used in this code is particulary usefull here, due to the strong discontinuity of the density field at the surface of strange stars (cf. the top panel in Fig. 2). Adapting the grids to the stellar surface allows to avoid the severe Gibbs phenomenon that such a discontinuity would necessary generate when performing polynomial expansions of the fields [52].

The hydrodynamical part of the code has been amended for the present purpose, namely to solve Eq. (19) for the velocity potential Ψ subject to the boundary condition (30). Let us recall that in the original version of the code, the treatment of Eq. (19) was different due to the vanishing of the density field at the stellar surface (see Appendix B of Ref. [46]).

We have used one numerical domain for each star and 3 (resp. 4) domains for the space around them for a small (resp. large) separation. In each domain, the number of collocation points of the spectral method is chosen to be $N_r \times N_\theta \times N_\varphi = 25 \times 17 \times 16$, where N_r, N_θ, and N_φ denote the number of collocation points (= number of polynomials used in the spectral method) in the radial, polar, and azimuthal directions respectively. The accuracy of the computed relativistic models has been estimated using a relativistic generalization of the virial theorem [36] (see also Sec. III.A of Ref. [4]). The virial relative error is a few times 10^{-5} for the closest configurations.

B. Evolutionary sequences

For each EOS we construct an *evolutionary sequence*, i.e. a sequence of quasi-equilibrium configurations with fixed baryon mass and decreasing separation. Such a sequence is expected to approximate pretty well the true evolution of binary neutron stars, which is entirely driven by the reaction to gravitational radiation and hence occur at fixed baryon number and fluid circulation.

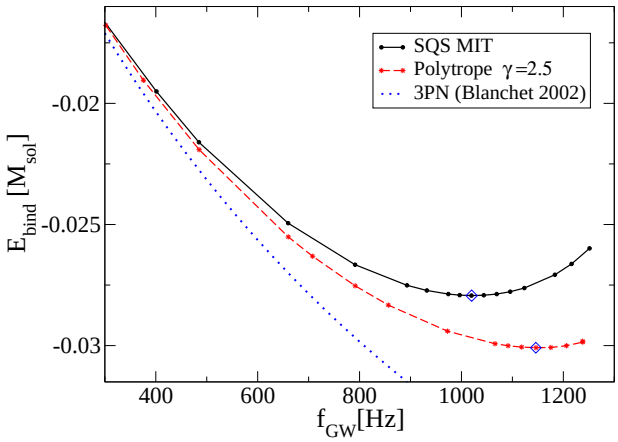

FIG. 3: Binding energy as a function of gravitational wave frequency along evolutionary sequences of corotating binaries. The solid line denotes strange quark stars, the dashed one neutron stars with polytropic EOS, and the dotted one point-mass binaries in the 3PN approximation [53]. The diamonds locate the minimum of the curves, corresponding to the innermost stable circular orbit; configurations to the right of the diamond are securaly unstable.

For a given rotational state we calculate evolutionary sequences of binary system composed of two identical neutron stars or two identical strange stars. The evolution of inspiraling corotating (irrotational) binaries is shown in Fig. 3 (Fig. 4). Fig. 3 and upper panel of Fig. 4 show the binding energy $E_{\rm bind}$ versus frequency of gravitational waves $f_{\rm GW}$ and lower panel of Fig. 4 show the total angular momentum of the systems as a function of $f_{\rm GW}$. The binding energy is defined as the difference between the actual ADM mass of the system, $M_{\rm ADM}$, and the ADM mass at infinite separation ($2.7\,M_\odot$ in our case). The frequency of gravitational waves is twice the orbital frequency, since it corresponds to the frequency of the dominant part $l = 2$, $m = \pm 2$. Solid and dashed lines denote quasi-equilibrium sequences of strange quark stars binaries and neutron stars binaries respectively. Dotted lines in Fig. 3 and Fig. 4 correspond to the 3rd PN approximation for point masses derived by [53]. Finally in Fig. 7 we compare our results with third order post-Newtonian results for point-mass particles obtained in the effective one body approach by Damour et al. 2000 [54], Damour et al. 2002 [55] and in the standard non-resummed post-Newtonian framework by Blanchet 2002 [53].

A turning point of $E_{\rm bind}$ along an evolutionary sequence indicates an orbital instability [36]. This instability originates both from relativistic effects (the well-known $r = 6M$ last stable orbit of Schwarzschild metric) and hydrodynamical effects (for instance, such an instability exists for sufficiently stiff EOS in the Newtonian

regime, see e.g. [49] and references therein). It is secular for synchronized systems and dynamical for irrotational ones.

In the case where no turning point of $E_{\rm bind}$ occurs along the sequence, the mass-shedding limit (Roche lobe overflow) marks the end of the inspiral phase of the binary system, since recent dynamical calculations for $\gamma = 2$ polytrope have shown that the time to coalescence was shorter than one orbital period for configurations at the mass-shedding limit [19, 28]. Thus the physical inspiral of binary compact stars terminates by either the orbital instability (turning point of $E_{\rm bind}$) or the mass-shedding limit. In both cases, this defines the *innermost stable circular orbit (ISCO)*. The orbital frequency at the ISCO is a potentially observable parameter by the gravitational wave detectors, and thus a very interesting quantity.

C. Corotating binaries

Quasi-equilibrium sequences of equal mass corotating binary neutron stars and strange stars are presented in Fig. 3. For both sequences we find a minimum of the binding energy. In the present rotation state, this locates a secular instability [36]. The important difference between neutron stars and strange stars is the frequency at which this instability appears. Indeed, there is a difference of more than 100 Hz: 1020 Hz for strange stars and 1140 Hz for neutron stars. The binding energy is the total energy of gravitational waves emitted by the system: a corotating binary strange star system emits less energy in gravitational waves and loses less angular momentum before the ISCO than a binary neutron star one with the same mass and compaction parameter in infinite separation.

Comparison of our numerical results with 3rd order PN calculations reveals a good agreement for small frequencies (large separations) (see Fig. 3 and 7). The deviation from PN curves at higher frequencies (smaller separation) is due to hydrodynamical effects, which are not taken into account in the PN approach.

D. Irrotational binaries

In Fig. 4 we present the evolution of the binding energy and angular momentum for irrotational sequences of binary neutron stars and strange stars. We also verify that these sequences are in a good agreement with PN calculations for large separations.

We note important differences in the evolution of binary systems consisting of strange stars or neutron stars. The strange star sequence shows a minimum of the binding energy at $f_{\rm GW} \simeq 1390$ Hz, which locates a dynamical instability [36] and thus defines the ISCO. The minimum of $E_{\rm bind}$ coincides with the minimum of total angular momentum J. This is in accordance with the "first law

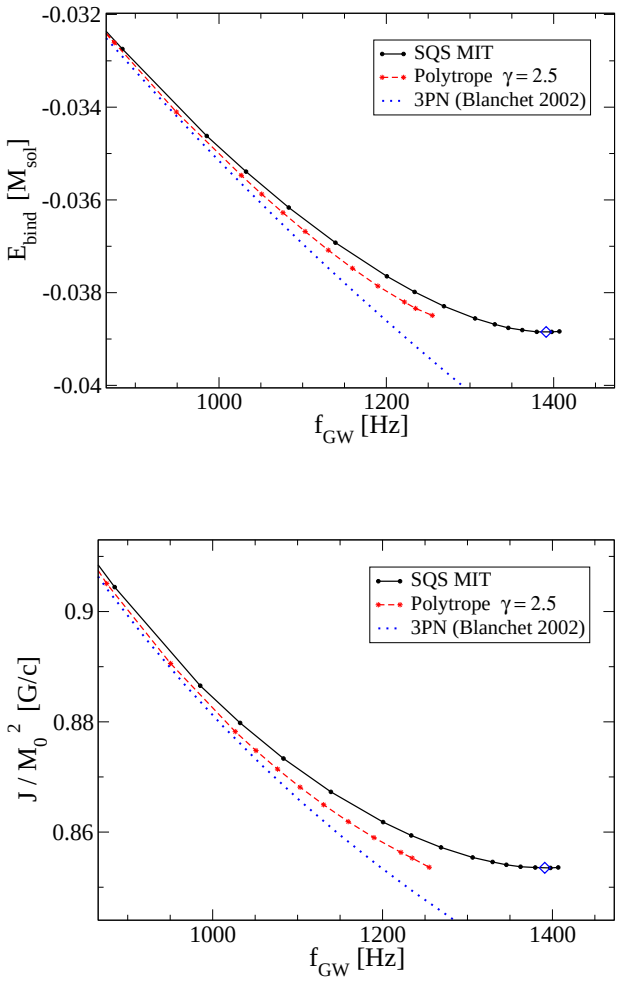

FIG. 4: Binding energy (top panel) and angular momentum (bottom panel) as a function of gravitational wave frequency along evolutionary sequences of irrotational binaries. The solid line denotes strange quark stars, the dashed one polytropic neutron stars, and the dotted one point-mass binaries in the 3PN approximation [53]. The diamonds correspond to dynamical orbital instability (the ISCO).

of binary relativistic star thermodynamics" within the IWM approximation as derived by Friedman, Uryu and Shibata [36] and which states that, along an evolutionary sequence,

$$\delta M_{\rm ADM} = \Omega \delta J. \qquad (31)$$

The surface of strange stars at the ISCO is smooth (see Fig. 5). On the contrary the neutron star sequence does not present any turning point of $E_{\rm bind}$, so that the ISCO in this case corresponds to the mass-shedding limit (final point on the dashed curves in Fig. 4). The gravitational wave frequency at the ISCO is much lower for neutron star binaries than for strange star binaries.

As already mentioned the adiabatic index in the outer layers of a compact star in a binary system plays a crucial role in its evolution, especially in setting the mass-

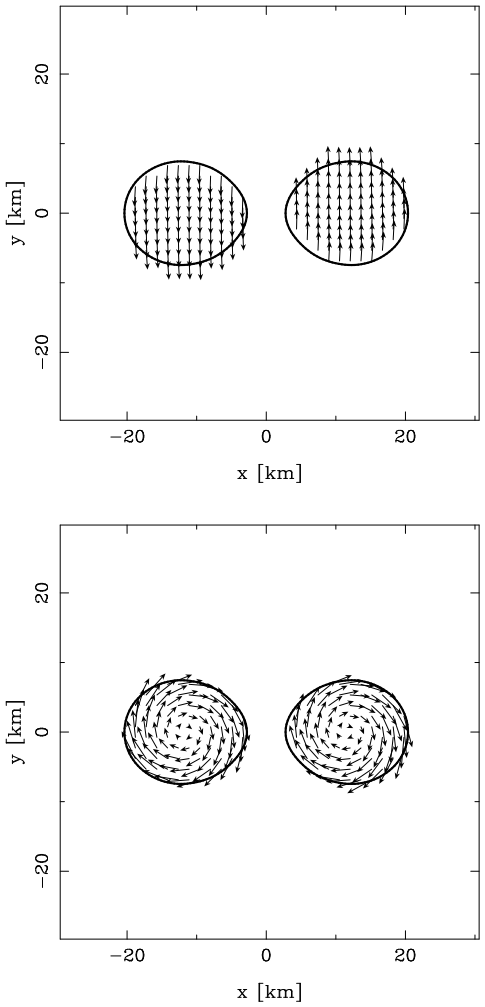

FIG. 5: Internal velocity fields of irrotational strange quark stars binaries at the ISCO. *upper panel:* velocity $\boldsymbol{U}$ in the orbital plane with respect to the "inertial" frame (Eulerian observer); *lower panel:* velocity field with respect to the corotating frame. The thick solid lines denote the surface of each star.

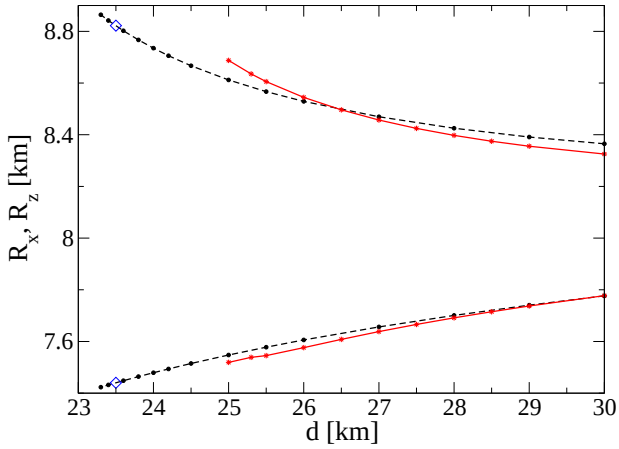

FIG. 6: Coordinate "radius" (half the coordinate size of a star in fixed direction) versus coordinate separation for irrotational quasi-equilibrium sequences of binary strange stars (solid line) and neutron stars (dashed line). Upper lines correspond to equatorial radius R_x (radius along the x axis going through the centers of stars in a binary system) and lower lines are polar radius R_z (radius along the rotation axis).

shedding limit. Although the crust of a $1.35\,M_\odot$ neutron star contains only a few percent of the stellar mass, this region is easily deformed under the action of the tidal forces resulting from the gravitational field produced by the companion star. The end of inspiral phase of binary stars strongly depends on the stiffness of matter in this region. It has been shown that the turning-point orbital instability for irrotational polytropic neutron stars binaries can be found only if $\gamma \geq 2.5$ and if the compaction parameter is smaller than certain value ([4], [25]). In fact, as shown in Fig. 31 of paper [4], they didn't find ISCO for irrotational binary neutron stars with $\gamma = 2.5$ or $\gamma = 3$ for compaction parameter as high as $M/R = 0.187$.

In Fig. 6 we present the evolution of two different stellar radii: the *equatorial radius* R_x, defined as half the diameter in the direction of the companion and the *polar radius*, defined as half the diameter parallel to the rotation axis. For spherical stars $R_x = R_z$. We see that at the end of the inspiral phase, neutron stars are, for the same separation, more oblate (more deformed) than strange stars. Binary neutron stars reach the mass-shedding limit (the point at which they start to exchange matter - a cusp form at the stellar surface in the direction of the companion) at coordinate separation $d \sim 25$km. We don't see any cusps for strange stars even for distances slightly smaller that the distance corresponding to the ISCO ~ 23.5 km.

It is worth to remind here the results on rapidly rotating strange stars and neutron stars. The Keplerian limit is obtained for higher oblatness (more deformed stars), measured for example by the ratio of polar and equatorial radius, in the case of strange stars than in the case of neutron stars [42, 56, 57, 58, 59, 60].

The differences in the evolution of binary (or rotating) strange stars and neutron stars stem from the fact that strange stars are principally bound by another force than gravitation: the strong interaction between quarks.

As already mentioned the frequency of gravitational waves is one of potentially observable parameters by the gravitational wave detectors. We can see from Fig. 7 that the 3rd PN approximations for point masses derived by different authors are giving ISCO at very high frequencies of gravitational waves > 2 kHz. Since in the hydrodynamical phase of inspiral the effect of a finite size of the star (e.g. tidal forces) is very important we see deviation of our numerical results from point-masses calculations. The frequency of gravitational waves at the ISCO strongly depends on equation of state and the ro-

tational state. For irrotational equal mass (of 1.35 $M_\odot$ at infinite separation) strange stars binaries described by the simple MIT bag model this frequency is $\sim$ 1400Hz and for neutron stars binaries described by four different realistic EOS it is between 800Hz and 1230Hz [5, 6].

VI. SUMMARY AND DISCUSSION

We have computed evolutionary sequences of irrotational and corotating binary strange stars by keeping the baryon mass constant to a value that corresponds to individual gravitational masses of 1.35 $M_\odot$ at infinite separation. The last orbits of inspiraling binary strange stars have been studied in the quasi-equilibrium approximation and in the framework of Isenberg-Wilson-Mathews approximation of general relativity. In order to calculate hydrodynamical phase of inspiraling irrotational strange stars binaries, i.e. assuming that the fluid has zero vorticity in the inertial frame, we found the boundary condition for the velocity potential. This boundary condition is valid for both the case of non-vanishing (e.g. self-bound matter) and vanishing density at the stellar surface (neutron star matter). In our calculations strange stars are built by strange quark matter described by the simplest MIT bag model (assuming massless and non-interacting quarks).

We have located the end of each quasi-equilibrium sequence (ISCO), which corresponds to some orbital instabilities (the dynamical instability for irrotational case or the secular one for synchronized case) and determined the frequency of gravitational waves at this point. This characteristic frequency yields important information about the equation of state of compact stars and is one of the potentially observable parameters by the gravitational wave detectors. In addition, the obtained configurations provide valuable initial conditions for the merger phase. We found the frequency of gravitational waves at the ISCO to be $\sim$ 1400 Hz for irrotational strange star binaries and $\sim$ 1000 Hz for synchronized case. The irrotational case is more realistic since the viscosity of strange star matter is far too low to ensure synchronization during the late stage of the inspiral. For irrotational equal mass (of 1.35 $M_\odot$) neutron star binaries described by realistic EOS [5, 6] the frequency of gravitational waves at the ISCO is between 800Hz and 1230Hz, much lower than for a binary strange quark star built of self-bound strange quark matter. We have considered only strange quark stars described by the simple MIT bag model with massless and non-interacting quarks. In order to be able to interpret future gravitational-wave observations correctly it is necessary to perform calculations for different strange star EOS parameters (taking also into account the existence of a thin crust) and for large sample of neutron stars described by realistic equations of state. For some MIT bag model parameters one is able to obtain less compact stars than considered in the present paper. In this case the frequency of gravitational waves at the end of inspiral phase will be lower than obtained by us. It should be also taken into account that stars in a binary system can have different masses [30]. The case of binary stars (with equal masses and different masses) described by different strange quark matter models will be presented in a separate paper [61].

We have shown the differences in the inspiral phase between strange quark stars and neutron stars described by polytropic equation of state having the same gravitational mass and radius in the infinite separation. It was already shown by Bejger et al. 2005 [6] that the frequency of gravitational waves at the end point of inspiraling neutron stars described by several realistic EOS without exotic phases (such as meson condensates or quark matter) can be predicted, in a good approximation, by studying binaries with assumed polytropic EOSs with $\gamma = 2$ or 2.5. For realistic EOS and polytropes with $\gamma \leq 2.5$ [4, 25] a quasi-equilibrium irrotational sequence terminates by mass-shedding limit (where a cusp on the stellar surface develops).

We found that it wasn't the case for inspiraling strange star binaries which are self-bound objects having very large adiabatic index in the outer layer. For both synchronized and irrotational configurations, we could always find a turning point of binding energy along an evolutionary sequence of strange quark stars, which defines an orbital instability and thus marks the ISCO in this case. In the irrotational case for the same separation strange stars are less deformed than polytropic neutron stars and for the same ratio of coordinate radius R_x/R_z their surfaces are more smooth. A cusp doesn't appear on the surface of a strange star in a binary system even for separation corresponding to orbital instability. The frequency of gravitational waves at the end of inspiral phase is higher by 300 Hz for the strange star binary system than for the polytropic neutron star binaries. The differences in the evolution of binary (or rotating) strange stars and neutron stars stem from the fact that strange stars are principally bound by an additional force, strong interaction between quarks.

Acknowledgments

We thank our anonymous referee for helpful comments. Partially supported by the KBN grants 5P03D.017.21 and PBZ-KBN-054/P03/2001; by "Ayudas para movilidad de Profesores de Universidad e Invesigadores espanoles y extranjeros" from the Spanish MEC; by the "Bourses de recherche 2004 de la Ville de Paris" and by the Associated European Laboratory Astro-PF (Astrophysics Poland-France).

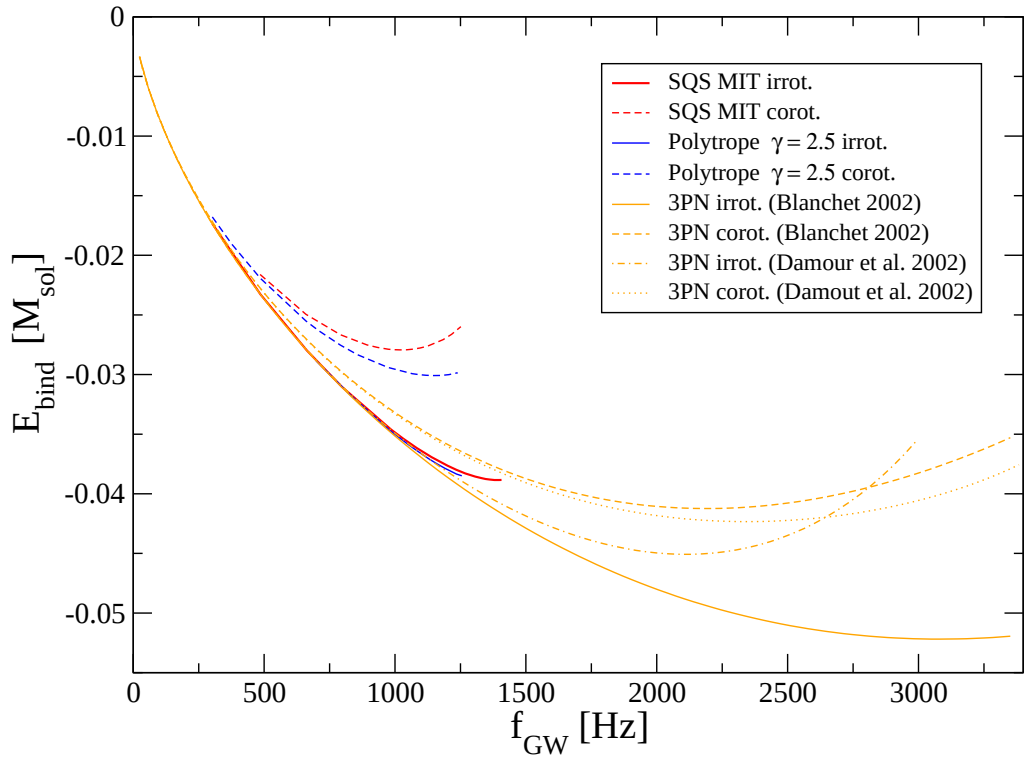

FIG. 7: Binding energy versus frequency of gravitational waves along evolutionary sequences of corotational (thick dashed lines) and irrotational (thick solid lines) equal mass (of 1.35 $M_\odot$) strange stars and polytropic neutron stars binaries compared with analytical results at the 3rd post-Newtonian order for point-masses by Damour et al. 2000 [54], Damour et al. 2002 [55] and Blanchet 2002 [53]

[1] V. Kalogera, C. Kim, D. R. Lorimer et al. Astrophys. J. **601**, 179 (2004).
[2] K. Belczynski, V. Kalogera, and T. Bulik Astrophys. J. **572**, 407 (2002).
[3] J. A. Faber, P. Grandcleḿent, F. A. Rasio, and K. Taniguchi, Phys. Rev. Let. **89**, 231102 (2002).
[4] K. Taniguchi and E. Gourgoulhon, Phys. Rev. D **68**, 124025 (2003).
[5] R. Oechslin, K. Uryu, G. Poghosyan, and F.K. Thielemann, Mon. Not. R. Astron. Soc. **349**, 1469 (2004).
[6] M. Bejger, D. Gondek-Rosińska, E. Gourgoulhon, P. Haensel, K. Taniguchi, and J. L. Zdunik, Astron. Astrophys. **431**, 297 (2005).
[7] P. Haensel, in *Final Stages of Stellar Evolution*, edited by J.-M. Hameury and C. Motch, EAS Publications Series vol. 7, 249 (EDP Sciences, Les Ulis, 2003).
[8] A. R. Bodmer, Phys. Rev. D **4**, 061601 (1971).
[9] E. Witten, Phys. Rev. D **30**, 272 (1984).
[10] P. Haensel, J.L. Zdunik, and R. Schaeffer, Astron. Astrophys. **160**, 121 (1986).
[11] C. Alcock, E. Farhi, and A. Olinto, Astrophys. J. **310**, 261 (1986).
[12] F. Weber, Prog. Part. Nucl. Phys. **54**, 193 (2005).
[13] J. Madsen, Lect. Notes Phys. **516**, 162 (1999).
[14] D. Gondek-Rosińska, E. Gourgoulhon, P. Haensel, Astron. Astrophys. **412**, 777 (2003).
[15] L. Blanchet, Living Rev. Relativity **5**, 3 (2002), `http://www.livingreviews.org/Articles/Volume5/2002-3blanchet/`
[16] T.W. Baumgarte, G.B. Cook, M.A. Scheel, S.L. Shapiro, and S.A. Teukolsky, Phys. Rev. Lett. **79**, 1182 (1997).
[17] S. Bonazzola, E. Gourgoulhon, and J.-A. Marck, Phys. Rev. Lett. **82**, 892 (1999).
[18] M. Shibata and K. Uryu, Phys. Rev. D **61**, 064001 (2000).
[19] M. Shibata and K. Uryu, Phys. Rev. D **64**, 104017 (2001).
[20] M. Shibata, K. Taniguchi, and K. Uryu, Phys. Rev. D **68**, 084020 (2003).
[21] K. Oohara and T. Nakamura, Prog. Theor. Phys. Suppl. **136**, 270 (1999).
[22] J.A. Faber, P. Grandclément, and F.A. Rasio, Phys. Rev. D **69**, 124036 (2004).
[23] P. Marronetti, G. J. Mathews, J. R. Wilson, Phys. Rev. D **60**, 087301 (1999).
[24] K. Uryu and Y. Eriguchi, Phys. Rev. D **61**, 124023 (2000).
[25] K. Uryu, M. Shibata, and Y. Eriguchi, Phys. Rev. D **62**, 104015 (2000).
[26] E. Gourgoulhon, P. Grandclément, K. Taniguchi, J.-A. Marck, and S. Bonazzola, Phys. Rev. D **63**, 064029

(2001)
[27] K. Taniguchi and E. Gourgoulhon, Phys. Rev. D **65**, 044027 (2002).
[28] P. Marronetti, M. D. Duez, S. L. Shapiro, T. W. Baumgarte, Phys. Rev. Lett. **92**, 141101 (2004).
[29] T. W. Baumgarte and S. L. Shapiro, Phys. Rep. **376**, 41 (2003).
[30] T. Bulik, D. Gondek-Rosińska, K. Belczynski, Mon. Not. R. Astron. Soc. **352**, 1372 (2004).
[31] D. R. Lorimer, Living Rev. Relativity **4**, 5 (2001), `http://www.livingreviews.org/Articles/Volume4/2001-5lorimer/`.
[32] Burgay, M., et al. Nature (London) , **426**, 531 (2003).
[33] L. Bildsten and C. Cutler, Astrophys. J. **400**, 175 (1992).
[34] C. S. Kochanek, Astrophys. J. **398**, 234 (1992).
[35] S. Bonazzola, E. Gourgoulhon, and J.-A. Marck, Phys. Rev. D **56**, 7740 (1997).
[36] J. L. Friedman, K. Uryu, and M. Shibata, Phys. Rev. D **65**, 064035 (2002).
[37] J. A. Isenberg : *Waveless approximation theories of gravity*, preprint University of Maryland, unpublished (1978).
[38] J. Isenberg and J. Nester, in *General Relativity and Gravitation*, edited by A. Held (Plenum, New York, 1980), Vol. 1.
[39] J.R. Wilson and G.J. Mathews, in *Frontiers in numerical relativity*, edited by C.R. Evans, L.S. Finn and D.W. Hobill (Cambridge University Press, Cambridge, England, 1989).
[40] K. Uryu, et al., in preparation (2005)
[41] E. Fahri, and R. L. Jaffe, Phys. Rev. D **30**, 2379 (1984)
[42] D. Gondek-Rosińska, T. Bulik, L. Zdunik, E. Gourgoulhon, S. Ray, J. Dey, and M. Dey, Astron. Astrophys. **363**, 1005 (2000)
[43] J. L. Zdunik, Astron. Astrophys. **359**, 311 (2000).
[44] E. Gourgoulhon, P. Haensel, D. Gondek, Astron. Astrophys., **294**, 747 (1995)
[45] D. Gondek, P. Haensel, and J. L. Zdunik, Astron. Astrophys., **325**, 217 (1997).
[46] E. Gourgoulhon, P. Grandclément, K. Taniguchi, J.A. Marck, and S. Bonazzola, Phys. Rev. D **63**, 064029 (2001).
[47] J. W. York, in *Sources of Gravitational Radiation*, edited by L. Smarr (Cambridge University Press, Cambridge, England, 1979).
[48] G. B. Cook, Living Rev. Rel. **3**, 5 (2000).
[49] K. Taniguchi, E. Gourgoulhon, and S. Bonazzola, Phys. Rev. D **64**, 064012 (2001)
[50] K. Taniguchi and E. Gourgoulhon, Phys. Rev. D **66**, 104019 (2002).
[51] `http://www.lorene.obspm.fr/`
[52] S. Bonazzola, E. Gourgoulhon, and J.-A. Marck, Phys. Rev. D **58**, 104020 (1998).
[53] L. Blanchet, Phys. Rev. D **65**, 124009 (2002).
[54] T. Damour, P. Jaranowski, and G. Schäfer, Phys. Rev. D **62**, 044024 (2000).
[55] T. Damour, E. Gourgoulhon, and P. Grandclément, Phys. Rev. D **66**, 024007 (2002)
[56] G. B. Cook, S. L. Shapiro, S. A. Teukolsky, Astrophys. J. **424**, 823, (1994)
[57] N. Stergioulas, W. Kluźniak, T. Bulik, Astron. Astrophys. **352**, L116 (1999)
[58] J.L. Zdunik, P. Haensel, D. Gondek-Rosińska, and E. Gourgoulhon, Astron. Astrophys. **356**, 612 (2000).
[59] P. Amsterdamski, T. Bulik, D. Gondek-Rosińska, and W. Kluźniak, Astron. Astrophys. **381**, L21 (2002)
[60] D. Gondek-Rosińska, N. Stergioulas, T. Bulik, W. Kluźniak, and E. Gourgoulhon, Astron. Astrophys. **380**, 190 (2001).
[61] D. Gondek-Rosińska and F. Limousin, in preparation (2005)